Combining Surface Plasmon Resonance and Quartz Crystal Microbalance for the in Situ Investigation of the Electropolymerization and Doping/Dedoping of Poly(pyrrole)

A. Bund,*,† A. Baba,‡ S. Berg,‡ D. Johannsmann,§ J. Lübben,‡ Z. Wang,§ and W. Knoll‡

Institute of Physical Chemistry and Electrochemistry, Dresden University of Technology, Mommsenstrasse 13, D-01062 Dresden, Germany, Max Planck Institute for Polymer Research, Ackermannweg 10, 55128 Mainz, Germany, Institute of Physical Chemistry, Arnold-Sommerfeld-Strasse 4, 38678 Clausthal-Zellerfeld, Germany

Received: January 8, 2003; In Final Form: April 10, 2003

An in situ combination of surface plasmon resonance (SPR) spectroscopy and quartz crystal microbalance (QCM) is used to study the electropolymerization and the doping/dedoping behavior of thin poly(pyrrole) (ppy) films in aqueous solutions. A mixed anion and cation exchange behavior is observed. The mass as determined with the QCM continuously increases during redox cycling. The combined QCM/SPR data reveal that this is caused by a relatively slow process occurring when ppy is in the oxidized (polaronic) state. This behavior is interpreted as an accumulation of neutral salt and solvent in the film.

Introduction

Conducting polymers are promising candidates for a variety of applications such as antistatic coatings, sensor layers, or matrixes for catalyst particles.[1,2] Many of these applications make use of the fact that the electric conductivity of the polymer can be controlled by its redox state. Poly(pyrrole) (ppy) is insulating or semiconducting in the reduced state and a metallic conductor ("synthetic metal") in the oxidized form. Upon oxidation, positive charges in the polymer chain are generated, which are compensated by the incorporation of anions (doping process).[3,4]

Given their complex behavior, it is desirable to have as much information available on these films as possible. Because there is considerable variability between different samples (for instance, induced by surface roughness), one wishes to combine complementary techniques in situ on the same sample. The combination of the quartz crystal microbalance (QCM) and surface plasmon resonance (SPR) spectroscopy provides such an approach.[5] Furthermore, it has been shown by SPR imaging that conducting polymer layers with thicknesses in nanometer range can be used as DNA sensors[6] or as a matrix for the electrocatalysis of redox enzymes.[7] When applied as thickness monitors, QCM and SPR yield an "acoustic thickness" and an "optical thickness", respectively. Here, we apply this concept to the doping/dedoping characteristics of conducting polymers.

Theory

Surface plasmon resonance (SPR) spectroscopy is a widely used method for the determination of optical thickness.[8] A metal−dielectric interface supports a surface mode of electromagnetic radiation, which decays exponentially into both the dielectric medium and the metal. Along the surface, the "surface plasmon" propagates with a certain wave vector, k_x. The propagation constant k_x very sensitively depends on the refractive index of the dielectric medium and changes when a film is present at the metal−air interface. To excite the surface plasmon, the k_x vectors of the plasmon and the incident beam have to be matched. This is achieved either by prism coupling or with a diffraction grating at the sample surface. The coupling condition is only fulfilled at a certain angle of incidence, which is the coupling angle. At this incidence angle, the reflectivity curve has a sharp minimum. SPR spectroscopy amounts to a precise measurement of the angle of minimum reflectivity.

One can show that the shift of the surface plasmon coupling angle, θ_c, induced by deposition of a film obeys the relation[9]

$$\frac{n\omega}{c}\Delta(\sin\theta_c) = \Delta k_x \approx \frac{\omega}{c}\frac{2\pi}{\lambda}\left(\frac{\epsilon_m\epsilon_a}{\epsilon_m+\epsilon_a}\right)^2 \frac{1}{\sqrt{-\epsilon_m\epsilon_a}(\epsilon_a-\epsilon_m)}\frac{(\epsilon_f-\epsilon_a)(\epsilon_f-\epsilon_m)}{\epsilon_f} d_{op,f} \quad (1)$$

n being the refractive index of the ambient medium,[10] ω the angular frequency, c the speed of light, θ_c the coupling angle, k_x the wave vector along the propagation axis, $\epsilon^* = \epsilon' + i\epsilon''$ the complex dielectric constant, $d_{op,f}$ the optical film thickness, and λ the wavelength. The indices a, f, and m denote the ambient medium, the film, and the metal substrate, respectively. Unfortunately, the dielectric constant ϵ_f of a polymer film is often not known a priori. A further problem with the practical use of eq 1 is the fact that the determination of the coupling angle θ_c usually involves an angle scan and therefore is inherently slow. Restricting the measurement to the reflectivity at a fixed angle on the slope of the reflectivity dip (Figure 1, arrow), one can obtain a time resolution well below 1 s. However, the analysis in this case remains qualitative because a change in reflectivity on the slope of the plasmon may be caused not only by a shift in the coupling angle but also by absorption, scattering, etc. However, one can still judge whether a film increases or decreases in optical thickness.

The QCM is based on the fact that the resonance frequency of a piezoelectric quartz plate decreases if a layer is deposited at its surface. Employing impedance analysis,[11] one monitors both the shift of the resonance frequency, δf, and the change of

* To whom correspondence should be addressed. Phone: +49 (0)351 463 34351. Fax: +49 (0)351 463 37164. E-mail: andreas.bund@chemie.tu-dresden.de.

† Dresden University of Technology.

‡ Max Planck Institute for Polymer Research.

§ Institute of Physical Chemistry.

10.1021/jp034043o CCC: $25.00
Published on Web 06/19/2003

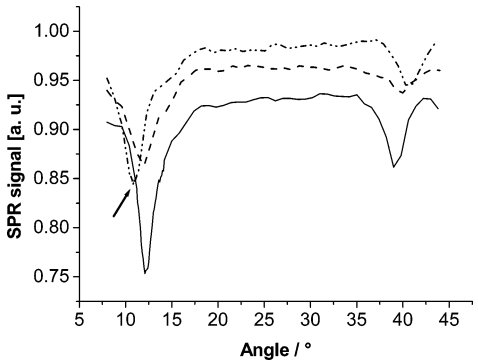

Figure 1. SPR spectra of the original quartz without film (—) and with a thin ppy film in the reduced (– – –) and the oxidized state (– · –). The arrow indicates the measuring angle for the SPR measurements at fixed angle.

the half-band half-width, $\delta\Gamma$, of the resonance curve of the quartz. Γ is directly related to the dissipation.[12] If the film thickness is much less than the wavelength of sound, a relation similar to eq 1 holds for QCM measurements:[13,14]

$$\frac{\delta f^*}{f} \approx \frac{m_f}{m_q}\left[\frac{Z_f^2 - Z_a^2}{Z_f^2}\right] = -\frac{\rho_f}{m_q}\left[\frac{Z_f^2 - Z_a^2}{Z_f^2}\right] d_{ac,f} \qquad (2)$$

The quantity δf^* is the complex frequency shift $\delta f + i\delta\Gamma$ of the quartz. The variables m_f and m_q are the mass per unit area of the film and quartz plate, respectively. Furthermore, $m_q = Z_q/(2f_0)$, f_0 being the fundamental resonance frequency of the unloaded quartz. Z_a, Z_f, and Z_q are the acoustic impedances of the ambient medium (the liquid), the film, and the quartz, respectively (here $Z_q = 8.8 \times 10^6$ kg m^{-2} s^{-1}). The acoustic impedance is given by $Z = i(\rho G^*)^{1/2} \tanh[(\rho/G^*)^{1/2})\omega d_{ac,f}$, ρ being the density and G^* the complex shear modulus. The acoustic impedance is the acoustic analogue of the refractive index; Z^2 is the analogue of the dielectric constant. We define the acoustic thickness, $d_{ac,f}$ (eq 3), as the thickness of a hypothetical "compact layer". A compact layer in this context is defined as a layer the acoustic impedance of which is much larger than the impedance of the liquid. In this case, the term in square brackets in eq 2 is unity and one has

$$d_{ac,f} = \frac{m_f}{\rho_f} = -\frac{\delta f}{f}\frac{m_q}{\rho_f} = -\frac{\delta f}{f}\frac{Z_q}{2f_0\rho_f} \qquad (3)$$

Equation 3 is the well-known Sauerbrey equation,[15,16] where δf is a real quantity indicating that smooth, rigid films only decrease the resonance frequency without increasing the dissipation.

Comparing eqs 1 and 3, one might think that the information contained in surface plasmon resonances and quartz crystal resonances should be essentially the same. However, this is not the case. First, the contrast in acoustics is usually much larger than that in optics. While refractive indices generally vary in the range of a few percent, shear moduli may easily vary by orders of magnitude. In optics, the quantity $(\epsilon_f - \epsilon_m)(\epsilon_f - \epsilon_a)/\epsilon_f$ (defining the optical contrast, see eq 1) is smaller than unity and roughly proportional to the concentration. Therefore, the plasmon shift is approximately proportional to the *adsorbed amount*. In acoustics, on the contrary, the function $(Z_f^2 - Z_a^2)/Z_f^2$ (defining the acoustic contrast, see eq 2) easily saturates even for dilute adsorbates.[17] The acoustic thickness reaches the *geometric thickness* at rather low coverage and does not increase further upon densification of the film by prolonged adsorption. More pictorially speaking, if the adsorbate drags some solvent along in its shear movement, the trapped amount of solvent appears as part of the film.[18] Swelling therefore effectively increases the acoustic thickness, while it affects the optical thickness to a much lesser degree.

In a recent paper, electrochemical measurements were introduced into combined QCM/SPR measurements as a third way of characterizing the sample. The electropolymerization of pyrrole was studied by tracking the frequency shift of a QCM and the reflectivity in SPR setup at the same time.[19] Here, we extend the investigation to the doping/dedoping behavior of thin ppy films (5−10 nm).

In electrochemical QCM experiments, the areal mass density m_f can be calculated from $m_f = \rho_f d_{ac,f}$ and be related to the passed charge density Q.[20] In the case of the electropolymerization of a monomer M such as pyrrole, the theoretical value of the ratio m_f/Q can be calculated from eq 4.

$$\frac{m_f}{Q} = \frac{(M_M - 2M_H) + x_A M_A + x_S M_S + x_N M_N}{(2 + x_A)F} \qquad (4)$$

where M_M, M_A, M_H, M_S, and M_N are the molar masses of monomer, incorporated anion, hydrogen, solvent, and neutral salt, respectively, x_A, x_S, and x_N are the molar equivalents of doping anions, solvent, and neutral salt per monomer, and F is the Faraday constant (96 485 C mol^{-1}). The product of m_f/Q and the Faraday constant represents the mass change associated with the exchange of one mole of electrons and is sometimes called the apparent molar mass M_{app} involved in an electrochemical reaction.

In the case of ppy, transfer of solvent and coions has been clearly verified.[4] Reviewing the actual literature, one learns that $x_A \approx 0.3$ seems to be a reasonable value.[21,22] The parameters x_S and x_N strongly depend on the preparation conditions.[23]

If side reactions (reactions that consume charge but do not change the mass on the quartz, such as formation of soluble oligomers or cross-linking of the polymer chains) occur, the experimentally observed ratios m_f/Q will be lower than the theoretical values.

Experimental Section

For an in situ combination of SPR and QCM, the quartz surface must have a corrugation grating to achieve coupling of the incident laser light to the plasmon. In our case, the grating was produced by reactive ion beam etching (RIBE). A photoresist (Micropositiv Shipley 1805) with a thickness of 150 nm was spin-cast onto the quartz blank ($f_0 = 5$ MHz, Maxtek). A master grating with a pitch of 520 nm was produced by illuminating the photoresist with crossed laser beams of a He:Cd laser ($\lambda = 442$ nm).[24] The resulting structure was transferred to the quartz plates with an ion mill (RR.ISQ76 from Roth & Rau, Wüstenbrand, Germany). A mixture of Ar, CF_4, and O_2 (flow rates of 1.6, 1.2, and 0.8 sccm, respectively) was applied to the surface at an average energy of 0.6 keV for 60s. Atomic force microscopy (AFM) images showed that the resulting structures were rather rectangular with a depth of 25 nm and a pitch of 520 nm. Finally, a 5 nm Cr adhesion layer and a 200 nm Au layer were deposited on both sides of the quartz.

The SPR measurements for the synthesis and the doping/dedoping process of the polymer layers were performed at a fixed angle, which was chosen prior to the experiment from complete SPR spectra of the native Au electrode or the ppy film (Figure 1). The sample was mounted on a double goniometer (Huber 410A). A p-polarized HeNe laser beam ($\lambda = 632.8$ nm) enters the sample cell (made of Teflon) where it

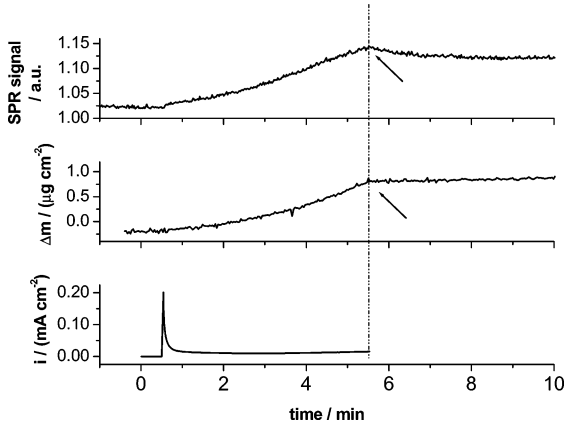

Figure 2. Current transient of ppy deposition from 0.1 M pyrrole, 0.1 M KCl, and accompanying changes of mass and reflectivity (10.5°) for potential step from OCP to 0.5 V (SCE) and back to OCP (arrow).

is coupled to the plasmon via the surface grating on the quartz. The reflected laser light is monitored by lock-in detection (EG&G 5209 lock-in amplifier). Data acquisition and control of the system electronics are accomplished using custom-made software.

The complex frequency shift δf^* (eq 2) of the quartz was determined by measuring the electrical admittance near the resonance frequencies of the quartz with a network analyzer (E5100A, Agilent Technologies). Details concerning the experimental setup can be found in ref 13. To separate the rf voltage (network analyzer) and the dc voltage (potentiostat), a combination of a capacitance and an inductance was used as described in ref 25.

An EG&G 263A potentiostat (Princeton Applied Research) controlled by the CorrWare Software (Scribner Associates, North Carolina) was used for the electrochemical experiments. One gold electrode of the quartz crystal (electrochemically active area 1.4 cm^2) served as the working electrode in a three-electrode arrangement. The counter electrode was a Pt foil (purity 99.99%, GoodFellow, Cambridge, England). All potentials were measured versus commercial reference electrodes: either a saturated calomel electrode, SCE, (Meinsberg Sensortechnik, Meinsberg, Germany) or a Ag/AgCl electrode (BAS scientific, Congleton, U.K.). In the text, potentials are quoted with respect to the SCE by taking into consideration the potential difference of 40 mV.

All solutions were prepared from analytical grade chemicals and ultrapure water (Milli-Q). The measuring cell was home-built from PTFE. Because of the limited space in the cell and in order not to block the optical path, inert gas purging was not applied.

Results

Synthesis of Thin ppy Films. The electropolymerization of pyrrole was initiated by stepping the potential from the open circuit potential (OCP) to +0.5 V(SCE) after 30 s. The current transient (Figure 2) shows the typical large peak due to double-layer charging. Afterwards the current density remains at $i \approx 7.5\ \mu A/cm^2$ and slowly increases after about 200 s. The cell was switched back to OCP after 332 s, at which i had reached a value of 16 $\mu A/cm^2$ (Figure 2, arrow). At that point, QCM indicated that a polymer layer with an areal mass density of approximately 1 $\mu g/cm^2$ had been deposited (Figure 2), which corresponds to a layer thickness of 6.7 nm assuming a polymer density of 1.5 g/cm^3.[26] Because the imaginary part of δf^* (eq 2) was only 50 Hz (measured at fifth harmonic), the Sauerbrey equation (eq 3) could be used to relate frequency shifts to mass changes. The electropolymerization was stopped at this relatively low thickness because the film absorbs at $\lambda = 633$ nm, and the plasmon becomes shallow. During the deposition, the reflectivity increased (Figure 2). Because the measurement was carried out an angle below the angle of minimum reflectivity, an increase of the reflectivity indicates an increase of the coupling angle and hence an increase of optical thickness. The increase of reflectivity should be proportional to the increase of the thickness, provided that the dielectric constant of ppy is constant during electropolymerization. After the current had been switched off, the frequency shift of the QCM immediately leveled off, whereas the reflectivity slowly decreased (Figure 2). Table 1 summarizes the resulting values of m_f (eq 3), Q, m_f/Q, and $x_S M_S + x_N M_N$ (eq 4) for two different ppy films, prepared under similar conditions. The electrical charges Q have been roughly corrected for the double-layer contribution by subtracting the charge determined from a potential step experiment with the native Au electrode in 0.1 M KCl (background measurement). These experiments also showed that there is no Au dissolution at the relatively moderate polymerization potential of 0.5 V (SCE). Because the expression $x_S M_S + x_N M_N$ is small for film 1, the incorporation of neutral salt and solvent seems to be absent. In the case of film 2, there is an additional net mass increase of about 11 g/faraday, which means that some solvent or neutral salt or both is incorporated during the electropolymerization. This limited reproducibility is often encountered with the electropolymerization of conducting polymer films.

TABLE 1: Results of the Electropolymerization of Two Different ppy Films[a]

film	m_f ($\mu g\ cm^{-2}$)	Q ($mC\ cm^{-2}$)	m_f/Q ($mg\ C^{-1}$)	$x_S M_S + x_N M_N$ ($g\ mol^{-1}$)
1	1.024	4.17	0.246	0.1
2	0.709	2.39	0.297	11.5

[a] m_f = areal mass density of the film as determined by the EQCM using eq 3; Q = passed electrical charge; $x_S M_S + x_N M_N$ = amount of solvent (S) and neutral salt incorporated into the film.

Characterization of Thin ppy Films. After the freshly prepared ppy films were washed several times with 0.1 M KCl, their doping/dedoping behavior was characterized by potential step and cyclic voltammetry (CV) in 0.1 M KCl. It must be noted that for the characterization of the ion-exchange behavior step experiments are better suited than CV experiments. Bruckenstein and Hillman point out that the response function in CV experiments is more complex and less readily interpreted.[27] As described above, the electrical charges have been corrected with the help of background measurements. Cathodic charges contain the contribution from both the double layer and the oxygen reduction reaction. The latter is difficult to account for, and it must be borne in mind that the correction procedure can introduce systematic errors.

The first reducing step (at −0.5 V (SCE)) was always accompanied by a mass decrease (Figure 3). Angle scans of the reflectivity (SPR spectra) showed that SPR can readily distinguish between the reduced (Figure 1, dashed line) and the oxidized state (Figure 1, dash-dotted line) of ppy. In the subsequent cycles, a continuous mass increase was observed (Figure 4). The damping of the quartz and therefore of the film did not change during the redox switching (Figure 5). In CV experiments, the same behavior was observed. The SPR signal followed the potential steps instantaneously. The mass increase with increasing cycle number was found in all experiments. In

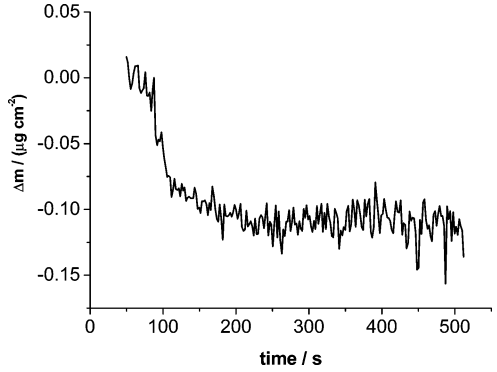

Figure 3. Mass change during the first reduction step (−0.5 V (SCE)) of a freshly prepared ppy film in 0.1 M KCl.

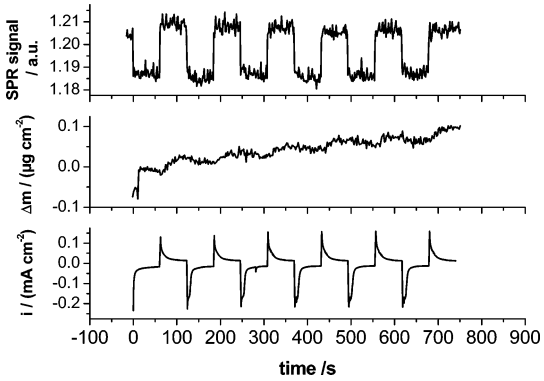

Figure 4. Current transients, mass change, and SPR signal of a thin ppy film accompanying a sequence of potential steps between −0.5 and 0.3 V (SCE).

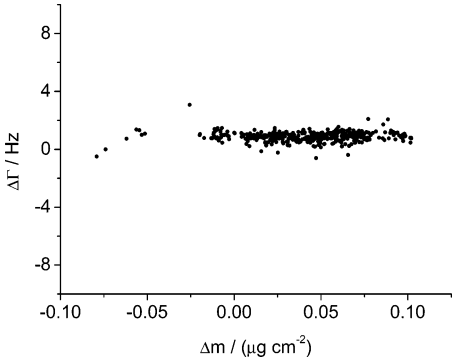

Figure 5. Damping change of the ppy film during the redox switching shown in Figure 4.

some cases, this behavior was accompanied by a weak decrease in the optical reflectivity, mostly occurring in the oxidized state.

Discussion

Electropolymerization of ppy. The results on the electropolymerization of ppy are in accordance with the previous study.[19] In that paper, a drift of the SPR signal after switching off the current (Figure 2, arrow) had also been observed and had been explained with relaxation processes in the polymer film. These processes cause a change in the dielectric constant and thus the SPR signal but no mass change. Because we observed no change of the dissipation of the quartz, the changes of the mechanical impedance Z_f (eq 2) and thus the complex shear modulus G^* accompanying the relaxation processes seem to be small.

Doping/Dedoping Behavior of Thin ppy Films. The first reduction steps of freshly prepared ppy films always showed mass decreases (Figure 3), corresponding to $M_{app} \approx -5$ g/mol. This value is definitely too small for a pure anion exchange, which would correspond to −35.5 g/mol (chloride). It is well-known that for ppy the apparent molar mass of the exchanged species depends on the preparation conditions[23] and the redox state (i.e., the actual potential).[4] In other words, ppy films can act as anion or cation exchange membranes or a combination of both. Transfer of solvent further complicates the situation. According to Gabrielli et al., the exchange of Cl^- has the smallest time constant for ppy films at −0.55 V (SCE). An exchange of Na^+ with two water molecules also occurs, but it is a little bit more sluggish. At 0.3 V (SCE), the redox reaction involves only the anion.[28] Obviously, in our case the ejection of anions (−35.5 g/mol) is counterbalanced by the ingress of cations (+39 g/mol, potassium) and the exchange of solvent (±18 g/mol, water). Bruckenstein et al. found that the transfer of the cation (sodium in their case) requires water transfer in the same direction,[29] and the work of Gabrielli shows that the number of solvent molecules transferred depends on the redox state of ppy with a tendency to higher hydration numbers in the cathodic state.[28] The constant damping behavior of the film during the redox switching (Figure 5) would indicate that the exchange of solvent (swelling and deswelling of the film) might play a minor role in our case. However, to further corroborate this statement more experiments are needed. One promising approach would be to include the determination of the frequency-dependent electrogravimetric transfer function, $\Delta m/\Delta E$.[30] It has been shown by Gabrielli et al. that this technique is capable of separating the individual contributions of solvent and ion transfer during redox cycling of conducting polymers.[28]

The increase of the reflectivity in the doping steps (Figure 4) could be interpreted as an increase of the film thickness. However, it must be borne in mind that the angle of minimum reflectivity in the SPR curve shifts to larger angles when the film is switched from the reduced to the oxidized state (Figure 1). Furthermore, the minimum reflectivity increases, indicating less energy transfer to the surface plasmon when the film is in the oxidized state. This shows that the imaginary part of the dielectric constant ϵ'' (cf. eq 1) increased with oxidation as a consequence of the formation of the polaronic band and the "metallic" state of oxidized ppy. In this study, the variation of the optical properties of the film during formation and doping/dedoping processes are particularly strong. Because the details of the variation of the dielectric constant ϵ_f with the state of the film are not known, we do not analyze our data quantitatively here.

At the moment, we cannot make detailed statements about the mechanism giving rise to the continuously increasing mass seen in Figure 4. It seems that the incorporation of cations and solvent become more and more dominating as the film is rapidly switched between its reduced and oxidized form. From the SPR data, we can conclude that the film is already in the oxidized (i.e., polaronic) state when the mass increase occurs. This would indicate that a neutral species is involved because the electroneutrality condition requires a fast exchange of charged species. From a thermodynamic point of view, this means either that the film is not in equilibrium after its preparation or that it changes its structure or reactivity or both during the doping/dedoping process.

Conclusions

Our work shows that the electrochemical in situ combination of QCM and SPR is a powerful tool for the investigation of doping/dedoping behavior of conducting polymer films. Future work will aim at a fine-tuning of the experimental conditions

(e.g., laser wavelength) and an analysis of the frequency dependence (transfer functions) of the individual signals. The aim is to extract more quantitative information from the SPR data such as the optical thickness and the dielectric constant of the film.

Acknowledgment. Part of this work was funded by the BMBF under Contract 03N 6500. A. Bund thanks the "Fonds der Chemischen Industrie" for financial support.

References and Notes

(1) Rodriquez, J.; Grande, H.-J.; Otero, T. F. Applications of Polymers. In *Handbook of Organic Conductive Molecules and Polymers: Conductive Polymers: Synthesis and Electrical Properties*; Nalwa, H. S., Ed.; John Wiley & Sons Ltd: New York, 1997; Vol. 2, Chapter VI, pp 457−460.

(2) Inzelt, G.; Pineri, M.; Schultze, J. W.; Vorotyntsev, M. A. *Electrochim. Acta* **2000**, *45*, 2403−2421.

(3) Li, Y. *J. Electroanal. Chem.* **1997**, *433*, 181−186.

(4) Gabrielli, C.; Garcia-Jareño, J. J.; Perrot, H. *Electrochim. Acta* **2001**, *46*, 4095−4103.

(5) Laschitsch, A.; Menges, B.; Johannsmann, D. *Appl. Phys. Lett.* **2000**, *77*, 2252−2254.

(6) Guedon, P.; Livache, T.; Martin, F.; Lesbre, F.; Roget, A.; Bidan, G.; Levy, Y. *Anal. Chem.* **2000**, *72*, 6003−6009.

(7) Raitman, O.; Katz, E.; Bückmann, A.; Willner, I. *J. Am. Chem. Soc.* **2002**, *124*, 6487−6496.

(8) Knoll, W. *Annu. Rev. Phys. Chem.* **1998**, *49*, 569−638.

(9) Pockrand, I. *Surf. Sci.* **1978**, *72*, 577−588.

(10) When prism coupling is used instead of grating coupling, n is the refractive index of the prism.

(11) Johannsmann, D.; Mathauer, K.; Wegner, G.; Knoll, W. *Phys. Rev. B* **1992**, *46*, 7808−7815.

(12) One has $\Gamma = {}^1/_2 D f_{res} = {}^1/_2 Q^{-1} f_{res}$, $D = Q^{-1}$ being the "dissipation" and Q the quality factor.

(13) Johannsmann, D. *Macromol. Chem. Phys.* **1999**, *200*, 501−516.

(14) Johannsmann, D. *J. Appl. Phys.* **2001**, *89*, 6356−6364.

(15) Sauerbrey, G. *Arch. Elektrotech. Übertragung* **1964**, *18*, 617−624.

(16) Sauerbrey, G. *Z. Phys.* **1959**, *155*, 206−222.

(17) Domack, A.; Prucker, O.; Rühe, J.; Johannsmann, D. *Phys. Rev. E* **1997**, *56*, 680−689.

(18) Martin, S. J.; Frye, G. C.; Ricco, A. J. *Anal. Chem.* **1993**, *65*, 2910−2922.

(19) Bailey, L. E.; Kambhampati, D.; Kanazawa, K. K.; Knoll, W.; Frank, C. W. *Langmuir* **2002**, *18*, 479−489.

(20) Bund, A.; Schneider, M. *J. Electrochem. Soc.* **2002**, *149*, E331−E339.

(21) Hillman, A. R.; Efimov, I.; Skompska, M. *Faraday Discuss.* **2002**, *121*, 423−439.

(22) Efinov, I.; Winkels, S.; Schultze, J. W. *J. Electroanal. Chem.* **2001**, *499*, 169−175.

(23) Zhou, M.; Pagels, M.; Geschke, B.; Heinze, J. *J. Phys. Chem. B* **2002**, *106*, 10065−10073.

(24) Mai, X.; Moshrefzadeh, R.; Gibson, U. J.; Stegeman, G. I.; Seaton, C. T. *Appl. Opt.* **1985**, *24*, 3155−3161.

(25) Bund, A.; Schwitzgebel, G. *Electrochim. Acta* **2000**, *45*, 3703−3710.

(26) Smela, E.; Kallenbach, M.; Holdenried, J. *J. Microelectromech. Syst.* **1999**, *8*, 373−383.

(27) Bruckenstein, S.; Hillman, A. R. *J. Phys. Chem. B* **1998**, *102*, 10826−10835.

(28) Gabrielli, C.; Garcia-Jareno, J.; Keddam, M.; Perrot, H.; Vicente, F. *J. Phys. Chem. B* **2002**, *106*, 3192−3201.

(29) Bruckenstein, S.; Brzezinska, K.; Hillman, A. R. *Electrochim. Acta* **2000**, *45*, 3801−3811.

(30) Gabrielli, C.; Garcia-Jareno, J.; Keddam, M.; Perrot, H.; Vicente, F. *J. Phys. Chem. B* **2002**, *106*, 3182−3191.